

g/l-Dispersion in interdigital micromixers with different mixing chamber geometries

Patrick Löb*, Helmut Pennemann, Volker Hessel

Chemical Process Engineering, Institut für Mikrotechnik Mainz GmbH, Carl-Zeiss-Str. 18–20, 55129 Mainz, Germany

Received 15 August 2003; accepted 28 November 2003

Abstract

The effect of mixing chamber geometry and feeding system geometry on g/l-dispersion in interdigital micromixers was basically investigated with regard to bubble size and bubble size distribution (BSD) using the systems nitrogen/aqueous glycerol solution with sodium dodecyl sulphate (SDS) as surfactant and nitrogen/water with SDS. The process of bubble formation was visually observed in glass micromixers with different mixing chamber geometries. This was set in correspondence to bubble size and BSD of the foams finally formed. Dependencies were deduced from comparing total flow rates, flow rate ratios and mixing chamber geometries. These investigations were supplemented by similar experiments with micromixers fabricated out of metal stainless steel. Based on the insight that a multi-channel gas feeding system without special measures for equipartition of the gas is counterproductive for small bubbles and narrow BSD, a new feeding system with generic flow configuration was developed and tested for the stainless steel micromixer. The feeding system was therefore simplified from a multi-channel gas feed system to a single-channel one. The single gas feed channel was encompassed from both sides by two liquid feed channels. It was shown that with this new feeding system smaller bubbles with a narrow size distribution are formed. © 2004 Elsevier B.V. All rights reserved.

Keywords: Interdigital micromixers; Multi-channel gas feed system; g/l-Dispersion

1. Introduction

One major driving force for applying microreactors in gas/liquid contacting is the improvement of mass transport between the two phases by providing high interfacial areas. This can be achieved via continuous (phases being separate, albeit in contact) or disperse (one phase finely distributed into the other) contacting. In the context of the latter means, this paper focuses on interdigital-feed microreactors. Interdigital microreactors are characterised by feeding structures leading to alternate lamellae arrangements of at least two fluids. Gas/liquid contacting relies here on a dispersion step to generate preferably small gas bubbles.

Micro-flow dispersion has attained considerable interest in the field of liquid/liquid contacting, not only due to achieving small droplets, but in particular concerning the respective size distribution which can be narrow [1] up to virtually delta-like (mono-disperse droplets) [2–4]. As a result of these and other fundamental experimentation works and theoretical descriptions [5–7], diverse applications of

disperse liquid/liquid reactions using micromixers have been meanwhile reported [8–11].

Compared to this work, today's level of knowledge on bubble dispersions in microreactors is not of the same depth. This is partly due to the fact that various tools for continuous gas/liquid contacting operation were developed as well and are now even commercially available, such as the falling film microreactors. Moreover, the reported dispersing works often focus on achieving slug-flow conditions, i.e. alternate bubble/liquid segment arrangements. Concerning the investigations on bubbly-flow generation, which is the content of this paper, a way to achieve mono-disperse bubbles using miniature nozzles is given in Ref. [12], albeit not relying on microfabrication techniques. A further study showed the capability of generating nearly mono-disperse bubble foams by an interdigital micromixer [13]. Later, reasonable mass transfer efficiency was indicated for the same device by measuring CO₂ absorption in alkaline aqueous solutions [14].

Interdigital microchannel arrays were first available as standard multi-purpose mixing version and from there modified for a specific purpose. To the latter group belong interdigital feed systems that differ in gas and liquid channels and which allow feed into individual channels. As one example, the microbubble column comprises single gas

* Corresponding author. Tel.: +49-61-31-990-375;

fax: +49-61-31-990-205.

E-mail address: loeb@imm-mainz.de (P. Löb).

feeding channels which are much smaller ($7\ \mu\text{m}$) than the liquid feeding channels ($20\ \mu\text{m}$) for reasons to intentionally increase the pressure drop in the gas channels and thereby to decrease the sensitivity of gas feeding to small pressure deviations between the channels. Nevertheless, no perfect equipartition was achieved [15,16].

Another differentiating factor of the specialty interdigital feed of the microbubble column is that each of the reaction channels (cross-section: $50\ \mu\text{m} \times 50\ \mu\text{m}$ or $300\ \mu\text{m} \times 100\ \mu\text{m}$) is fed by only one supply channel for the gas and one for the liquid from the interdigital feeding system [15,16]. The walls of the subsequent reaction channels prevent coalescence processes between bubbles formed at neighbored gas feeding channel outlets. Furthermore, the width and height of the reaction channels precisely determine bubble width and height. Different flow patterns like slug (Taylor) flow and annular flow were observed within the reaction channels depending on total flow rate and flow rate ratio [15,16].

Another specialty interdigital feed was reported by Jensen and coworkers [17–19]. The peculiarity comes from the connection of the parallel alternate channel to a packed bed, either composed of powder particles or of artificial microstructured columns. In particular for g/l/s processes, two such microfluidic devices were investigated. In the first type, porous catalyst particles in a packed bed arrangement are fixed by filter structures at the end of the reaction channel. In the second type, the reaction channel comprises an array of microstructured columns, covered with a thin layer of porous silicon as catalyst support. This simulates the structure of a packed bed, but with a much more precise definition of bed properties. A set of four channels for the gas and five channels for the liquid feed one reaction channel (cross-section: $625\ \mu\text{m} \times 300\ \mu\text{m}$) was employed. Among the observed flow patterns [17–19], a parallel flow of (non-uniform) bubbles with a diameter about $150\ \mu\text{m}$ was found in a reaction channel without packing for the system water/air [19].

Coming back to the standard interdigital flow configurations, IMM's standard slit interdigital micromixer made of stainless steel (SSIMM), equipped, e.g. with LIGA-type metallic inlay as feeding unit, is a multi-purpose tool used, first of all, for mixing of miscible liquids, mixing of gases, emulsion generation and forced precipitation of micro-scale solid particles as well as for g/l-contacting [20–22]. Concerning g/l-contacting in these devices, Hessel et al. reported basic investigations concerning the effects of fluid viscosity, flow rate ratio, total flow rate and modifications of the geometry of the mixing chamber on bubble size, and flow pattern were determined [13]. Because of the stainless steel housing, it was not possible to observe visually the bubble formation process in this device. Of special interest is that besides bubbly flow also the formation of very regular foam, showing a crystal-like packing, was observed. The corresponding flow of bubbles was termed "hexagon flow".

Using the same micromixer, Mathes and Plath focused their investigations on the formation of such regular foams

[23]. They showed that in the case of pressure driven fluid flows for a given g/l-system these regular foams are only formed in a narrow pressure range. The flowing foams produced by SSIMM are also the basis for serial catalyst screening in g/l-systems described by de Bellefon et al. [24–26].

In view of these first applications and the lack of knowledge on the underlying fundamentals regarding the hydrodynamics (as stated above), this article will try to answer the question how far multi-purpose tools, such as IMM's standard interdigital micromixers, are amenable to complex tasks such as gas/liquid-contacting. As it stands to reason that they will not exhibit ideal behaviour, this article also wants to show also which modifications are needed for that purpose.

2. Experimental

2.1. Materials

g/l-Dispersion formation in the glass mixers was investigated for the system nitrogen/aqueous glycerol solution (weight ratio of water/glycerol: 35/65; glycerol: anhydrous, purum, Fluka, order no. 49780) with sodium dodecyl sulphate as surfactant (10^{-2} mol/kg; purum, Fluka, order no. 71728). For better visualisation water blue (10^{-3} mol/kg; purum p.a., Fluka, order no. 95302) was added as dye to the aqueous solution. For the experiments with IMM's standard slit interdigital mixer (SSIMM) the system nitrogen/water with sodium dodecyl sulphate as surfactant (10^{-2} mol/kg) was used. Gas/liquid-contacting yields for these systems a foam stable at least for the time scale of the experiments. The investigated flow rates ranged from 60 ml/h to 180 ml/min for the gas and from 30 to 100 ml/h for the liquid.

2.2. Experimental setup

Fig. 1 shows the experimental setup with a glass micromixer incorporated. It consisted essentially in flow direction of feeding units, mixer and glass tube. A piston pump (KP2000; Desaga Sarstedt-Gruppe, Wiesloch, Germany; 10 ml pistons) was used to feed the liquid. The nitrogen flow was controlled by a mass flow meter (EL-Flow; Bronkhorst HI-TECH, Ruurlo, The Netherlands). Different micromixers were used. They are described below in detail. The inner diameter of the glass tube connected to the outlet of the mixers was 3 mm in the case of the experiments with the glass mixers and 2.2 mm in the case of the experiments with the stainless steel micromixers. The experiments were performed at ambient temperature.

2.3. Flow monitoring

The transparent glass micromixers allow direct observation of the process of foam formation at the outlet of the feeding channels itself and the bubble flow through the fluid

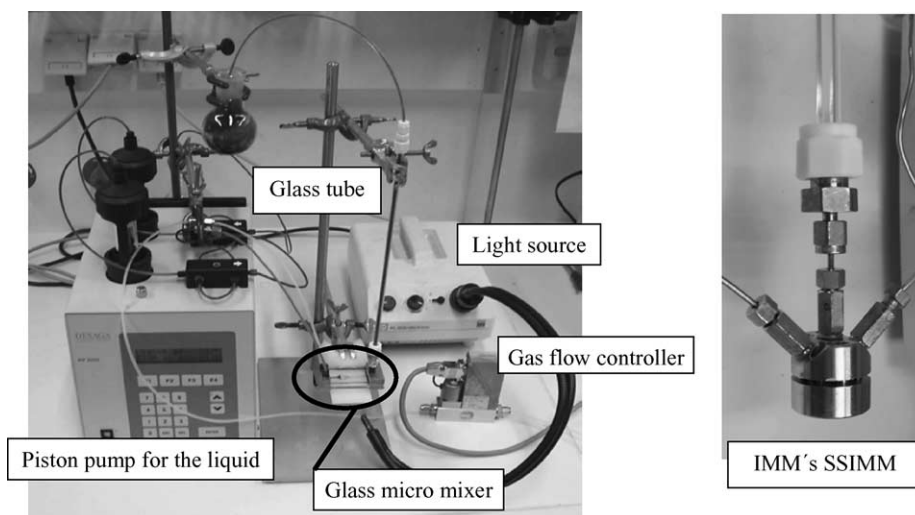


Fig. 1. Experimental setup for g/l -dispersion with an incorporated glass mixer (left). Instead of the glass mixer, also IMM's standard slit interdigital micromixer (SSIMM) can be integrated into the setup (right).

passage following the start of contacting, simply named mixing chamber in the following. Images were taken by using an analog camera mounted on a microscope (Olympus BX40 F-3; Olympus Optical Co. Ltd., Japan) fixed directly above the mixing chamber. The tube was connected to the mixer in order to get a fast qualitative impression on the formed foam in regard to bubble sizes and bubble size distribution (BSD). Images were taken here by a CCD camera (Sony 3CCD Color Video Camera/CCD-IRIS DXC-930 P; Sony Corporation, Japan) mounted on the same microscope as above but fixed lateral to the glass tube. Exact quantitative analyses were not performed here because of the optical distortion effect of the glass walls and because the visible parts of the foam may—based on unknown ordering effects in the foam in the tube—not represent the whole foam. In some cases one monolayer of the formed foam was collected directly at the outlet of the mixer on a glass microscope slide and analysed optically using the above-mentioned microscope and CCD camera. The bubbles diameter were then determined manually using a printout with calibrated length scale. By this method it was also checked that the mixer outlet, the adapters connecting mixer and tube and the tube did not change bubble sizes and BSD. Based on the exactness

of the analyses used no changes were observed. Instead of the glass micromixers also stainless steel micromixers were incorporated (see Fig. 1).

2.4. Interdigital micromixers used for the experiments

Two kinds of interdigital micromixers were used. The feeding structures for the two fluids consist either of co- or countercurrent flow interdigital array of microchannels (see Fig. 2). In the first case the feeding structures lie in the same plane as the mixing chamber and in the other case the mixing chamber is perpendicular to the plane with the feeding structures. The properties of all used mixers are listed in Table 1.

The three used glass micromixers have each a co-current flow interdigital array of microchannels. The fabrication is already described in detail elsewhere [27]. The mixers contain the same feeding system, but differ in the geometry of the mixing chamber with either rectangular, triangular or so-called slit-type shape (see Table 1). The latter shape represents a more complex geometry corresponding to the design of the mixing chamber realised in stainless steel as part of IMM's commercial standard slit interdigital micromixer

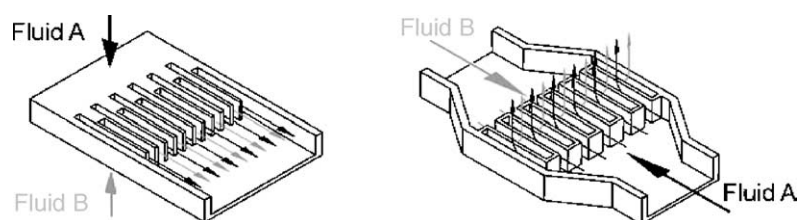
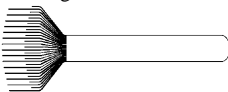
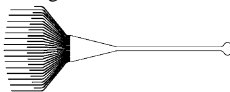
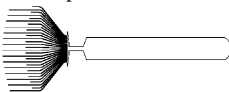
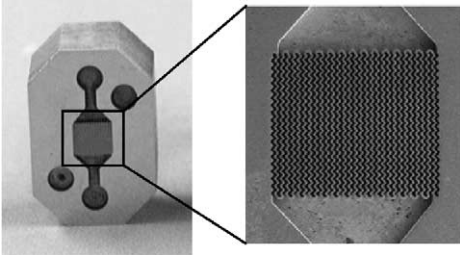
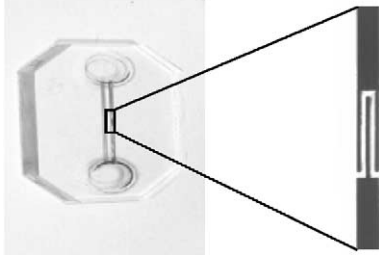


Fig. 2. Two types of interdigital micromixers. They have either a co-current flow microchannel array (left) or countercurrent flow microchannel array (right) as feeding structure. The latter is covered by a plate with a slit opening (not shown in the illustration) where the substreams of the fluids are contacted in an alternating way.

Table 1
Construction dimensions of micromixers used

Co-current flow interdigital (glass) micromixers ^a		
Rectangular ^b	Triangular ^c	Slit-shaped ^d
		
Countercurrent flow interdigital (steel) micromixers with slit-type mixing chamber geometry ^e		
Multi-channel gas feed system ^f	Single-channel gas feed system ^g	
		
Collecting slit width: 30, 60, 120 and 180 μm		

^a Common features: type of feeding structure: co-current flow interdigital multi-channel array; 2×15 feed channels with a width of $60 \mu\text{m}$, separated by walls with a width of $50 \mu\text{m}$; height of the feeding system and the flow through chamber: $150 \mu\text{m}$; width of the outlet region: $3250 \mu\text{m}$.

^b No constriction of chamber width.

^c Constriction of chamber width from 3250 to $500 \mu\text{m}$.

^d Collecting slit ends up in a short distance from the outlet region in a $500 \mu\text{m}$ broad channel which expands finally to a width of $3250 \mu\text{m}$.

^e Common features: type of feeding structure: countercurrent flow interdigital multi-channel array; principal geometry of the flow through chamber: collection slit spanning over the microchannel array followed by a $500 \mu\text{m}$ boring and thereafter a $3500 \mu\text{m}$ boring.

^f Height of the feeding system: $300 \mu\text{m}$; each 19 gas and liquid supply channels with a width of $25 \mu\text{m}$ separated by walls with a width of $25 \mu\text{m}$.

^g Height of the feeding system: $100 \mu\text{m}$; one gas supply channel with a width of $30 \mu\text{m}$ separated by walls with a width of $30 \mu\text{m}$ from two surrounding liquid feed channels also $30 \mu\text{m}$ width.

(SSIMM). For a better understanding, Fig. 3 shows an SEM image of the layer of the glass mixer bearing the feeding structures and an image of a cut through the mixing chamber of SSIMM. Both comprise the same generic flow configuration, namely a sequence of flow compression and expansion. Albeit the same in generic terms, the glass mixer is not a one-to-one replica of SSIMM since the planar structure of the glass mixers does not represent the three-dimensional form of the cylindrical boreholes.

SSIMM belongs to the class of mixers with countercurrent flow interdigital array of microchannels as feeding structure. Design and fabrication is already described in detail elsewhere [21]. Only features of the mixers essential for this work are described again in the following. The multi-channel array of the feeding structure, as schematically shown in Fig. 2 (right), was masked except for a small strap perpendicular to the direction of the incoming fluids, spanning over the complete width of the microchannel array. This strap is the starting point of the mixing chamber perpendicular to the multi-channel array with the geometry shown in Fig. 3 (bottom). The length of the strap in flow direction within the multi-channel array is called slit height in the following. Different versions of SSIMM were used. These are characterised by the slit height (30 , 60 , 120 or $180 \mu\text{m}$) and the used feeding structure (multi-channel or single-channel gas feeding).

The described micromixers (apart from the SSIMM version with the new single-channel gas feeding system) were already used for other investigations and applications and not specially designed for g/l-contacting.

2.5. New generic single-channel gas feeding structure

Up to now only multi-channel feeding structures were used in SSIMM. In the framework of this work a new generic single-channel gas feeding system was developed. As in the case of the multi-channel feeding system, the structure was sustained by a so-called inlay. The outer dimensions of the inlay and the principle arrangement of the fluidic structures on it were kept to assure compatibility of the new inlay to the SSIMM housing (see images of the inlays in Table 1). The central feeding structure was simplified and consists of an interdigital arrangement of two feeding channels for the liquid and only one for the gas. The precise dimension are given in Table 1. The material of the inlay is polycarbonate (macrolon[®], Bayer). Microstructuring was performed by laser ablation with an excimer laser (LPX 110i; Lamba-Physik, Göttingen, Germany; wavelength: 193 nm ; pulse width: 17 ns ; fluence: 1 J/cm^2) by static mask projection for the cylindrical structures and by dynamic mask projection for the channels.

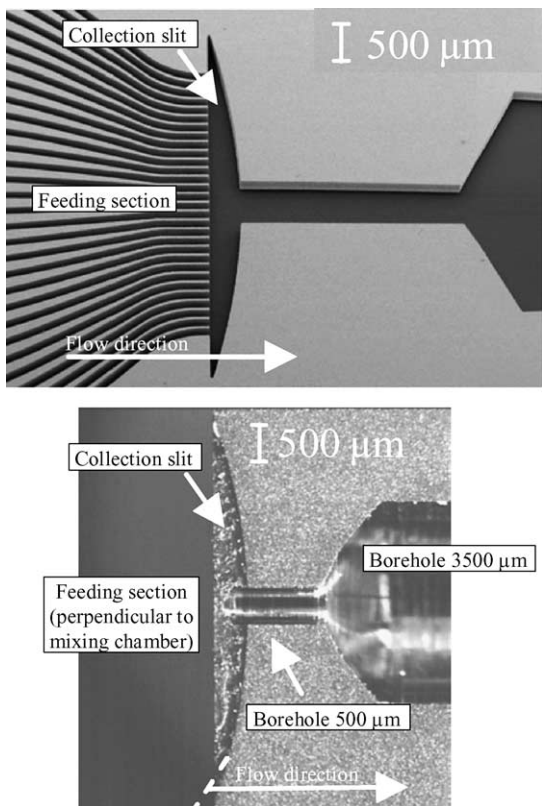


Fig. 3. Comparison of flow through chamber of slit-shaped glass micromixer and the flow through chamber in IMM's standard slit interdigital micromixer (pictures from a cut through the steel top housing part).

3. Results and discussion

Starting point were experiments with interdigital glass micromixers with different mixing chamber geometries allowing direct and visual observation of the bubble/foam formation. The same mixers have already been employed for investigations on mixing of liquids and on 1/1-dispersion [27]. Hereby, hydrodynamic features were found like the formation of regular fluidic assemblies, being composed of either lamellae or cylinders, and their subsequent geometric and hydrodynamic focusing, and the formation of droplets in the case of the 1/1-dispersion either directly at the outlet of the feeding channels or through break-up of cylinders in the mixing chamber dependent on flow ratio of the two fluids.

3.1. Foam formation in rectangular glass micromixer

In a first set of experiments foam formation in the rectangular glass micromixer was investigated in dependence of gas flow rate. The liquid flow rate was kept constant at 30 ml/h while the gas flow rate was increased from 60 to 180 ml/min. Looking at the foams formed in the glass tube connected to the outlet of the mixer (Fig. 4), already at first glance it can be stated that with increasing gas flow rate the bubble size distribution gets broader, whilst the average bubble size shifts to larger value. The underlying foam formation process was documented in images taken from the flow pattern within the mixing chamber (see also Fig. 4).

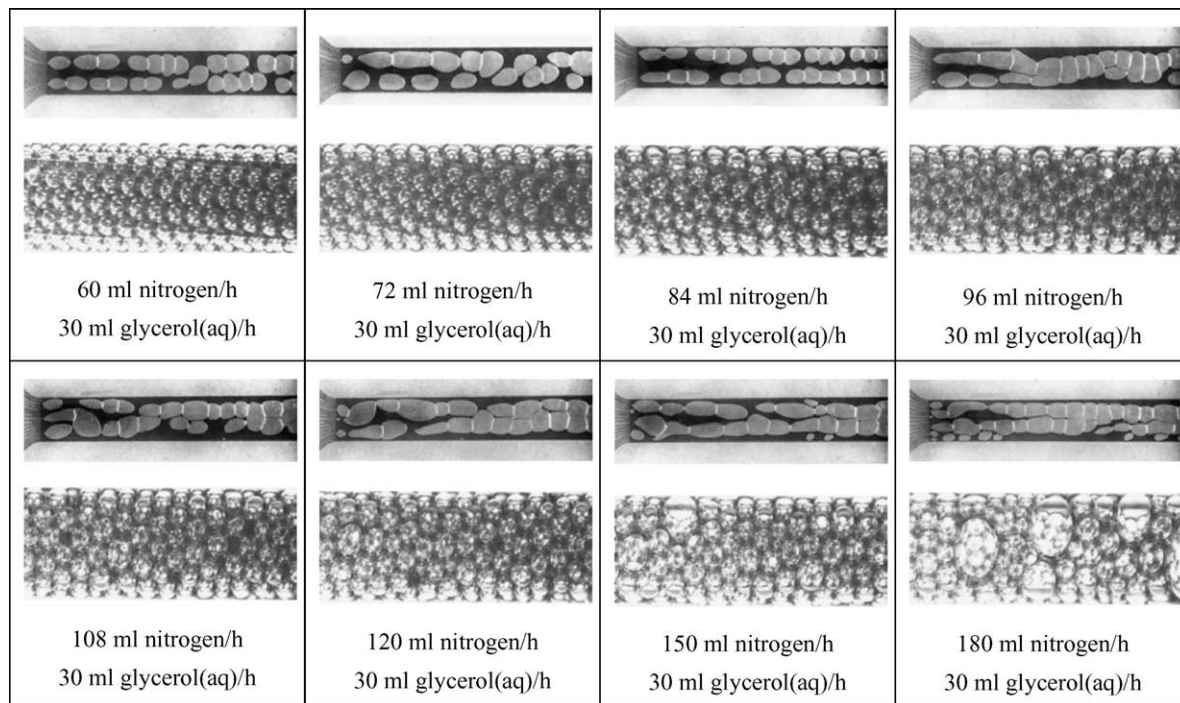


Fig. 4. Foam formation in rectangular glass mixer. The upper image of each set shows the flow through chamber, the lower image the glass tube connected to the mixer outlet. Liquid flow rate was kept constant at 30 ml/h, gas flow rate was varied from 60 to 180 ml/h.

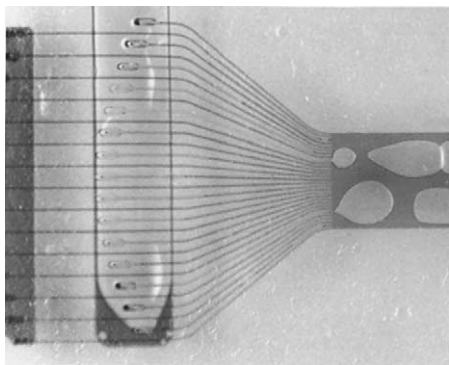


Fig. 5. Detail of feeding section of the rectangular glass mixer during g/l-dispersion.

Before providing a qualitative explanation on BSD based on these images, the fact that not all gas feeding channels are active during foam formation has to be considered in more detail. Fig. 5 shows the feeding section of the mixer in a magnified view exemplary for a gas flow rate of 72 ml/h and a liquid flow rate of 30 ml/h. Only 2 out of 15 gas feeding channels are active, the rest is flooded by the liquid in differing degree. The flooding of the channels indicates that capillary forces play a major role here in regard to equipartition. Capillary forces differ probably from channel to channel as consequence of small deviations in geometry and surface properties. This influence of capillary forces diminishes with increasing gas flow rate. This matches to the observation of increasing number of active gas feeding channels with higher gas flow rate (see Fig. 4). For the following discussion, it is also important that bubble formation at one channel is not independent from the bubble formation at another channel even there is no direct contact between the bubbles. Bubble pinch-off is connected to pressure changes in the affected channel which influences the other active gas channel.

Broadening of BSD with increasing gas flow rate can be attributed to several origins:

- increasing probability of steric restrictions between neighbored bubbles already during bubble formation;
- increasing probability of geometric side-wall restrictions on bubble formation;
- increasing probability of coalescence through collision in the mixing chamber;
- bubble formation gets more and more irregular, regarding time and location, and hence irreproducible with increasing amount of active gas channels due to commingling gas channels.

The sizes of the bubbles formed were measured for three gas flow rates (60, 120 and 180 ml/h). The corresponding diagram (Fig. 6) exhibits again the broadening of the BSD with increasing gas flow rate. Going from a gas flow rate of 60 to 120 ml/h broadening of the BSD is accompanied by an increase of the mean droplet diameter (from 547 to 663 μm). Although broadening continues going from 120 to 180 ml/h, the mean droplet diameter drops to 609 μm . Here, broadening does not only stem from the formation of increasing bigger bubbles, but also from formation of bubbles smaller than those accessible at low gas flow rates. This has to be attributed to the increased complexity of bubble formation for multiple channels being active, exhibiting dynamic and location changes.

In a second set of experiments with the rectangular glass micromixer, the total flow rate was increased, while the ratio of gas-to-liquid flow rate was kept constant (Fig. 7). With increasing total flow rate, the number of active channels rises which is again connected to a broadening of the BSD. But even for the highest total flow rate with a gas flow rate of 282 ml/h the size and amount of larger bubbles do not reach the respective values observed in the above discussed set of experiments. This may be attributed to two reasons. Firstly, the gas-to-liquid flow ratio is for higher total flow

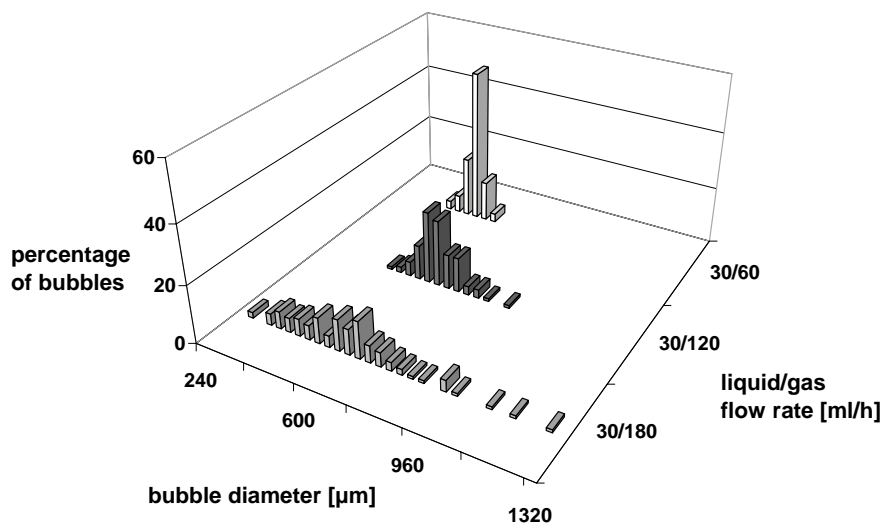


Fig. 6. Bubble size distribution for the rectangular glass mixer.

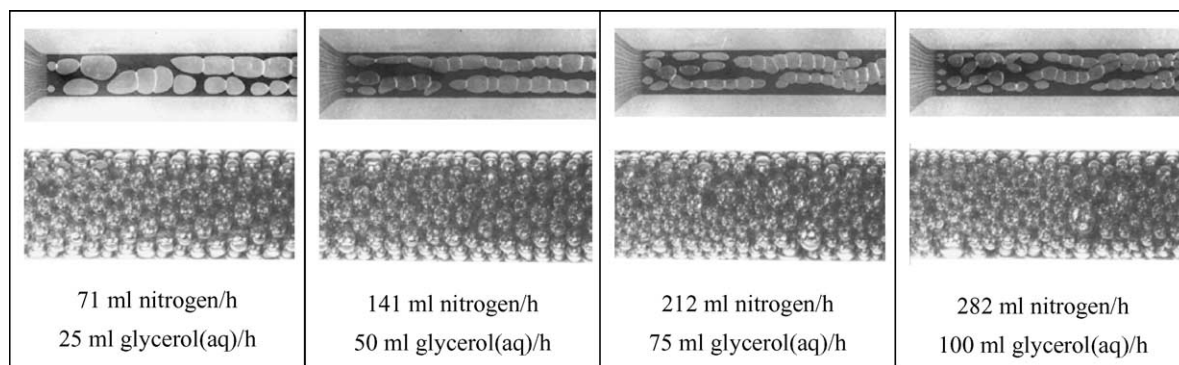


Fig. 7. Foam formation in rectangular glass mixer. The upper image of each set shows the flow through chamber, the lower image the glass tube connected to the mixer outlet. The flow rate ratio gas/liquid was kept constant while the total flow rate was increased.

rates smaller than in the first set of experiments, reducing the probability of collision of bubbles in the mixing chamber. Secondly, the liquid flow rates in the case of the higher total flow rates is greater than in the first set of experiments, facilitating bubble pinch-off.

3.2. Foam formation in triangular glass micromixer

In a set of experiments, foam formation in the triangular glass micromixer was investigated in dependence of gas flow rate in a similar fashion as for the rectangular glass micromixer. Again, the liquid flow rate was kept constant at 30 ml/h, while the gas flow rate was increased from 60 to 180 ml/min. Fig. 8 shows images of the bubble formation process and the formed foam for selected experiments and allows direct comparison to the foams formed with the rectangular glass micromixer. For none of the investigated flow rates, regular foams are produced. This is not surprising for higher gas flow rates (see images for 120 and

180 ml nitrogen/h), since the decreasing width of the mixing chamber in the triangular glass micromixer represents a geometric restriction leading to bubble contact during bubble formation and to bubble collision in the mixing chamber. Interestingly, also for a gas flow of 60 ml/h the formed foam exhibits already a broad BSD. This may be attributed to the process of bubble deformation necessary to pass the small channel after the focusing zone of the mixing chamber and of the passage of the bubbles through this channel itself. Probably, this process leads to time-dependent pressure changes affecting bubble formation.

Again for quantitative statements, the sizes of the bubbles formed were measured for three gas flow rates (60, 120 and 180 ml/h). The corresponding result diagram (Fig. 9) illustrated the broad BSD for all three gas flow rates. The calculated mean bubble size diameter increases with the gas flow rate: from 718 to 734 μm and finally to 789 μm whereby the major experimental error (precise detection of bubble surface) is estimated to be 15 μm .

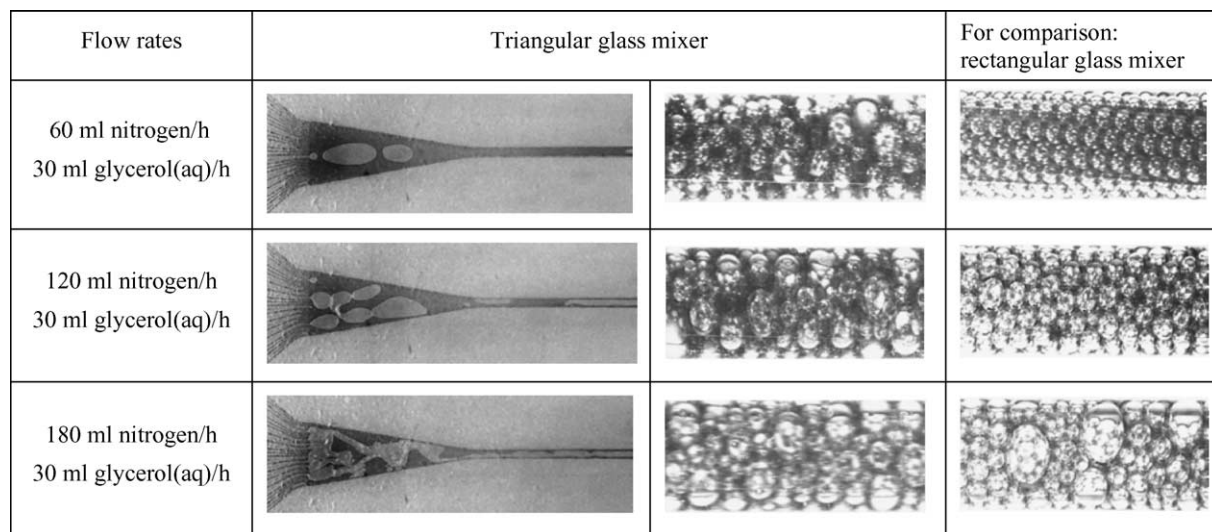


Fig. 8. Foam formation in triangular glass mixer. The left row of images show the flow through chamber, the middle row the glass tube connected to the mixer outlet. The right row shows as comparison the glass tube for the rectangular glass mixer. The liquid flow rate was kept constant at 30 ml/h while the gas flow rate was increased from 60 to 180 ml/h.

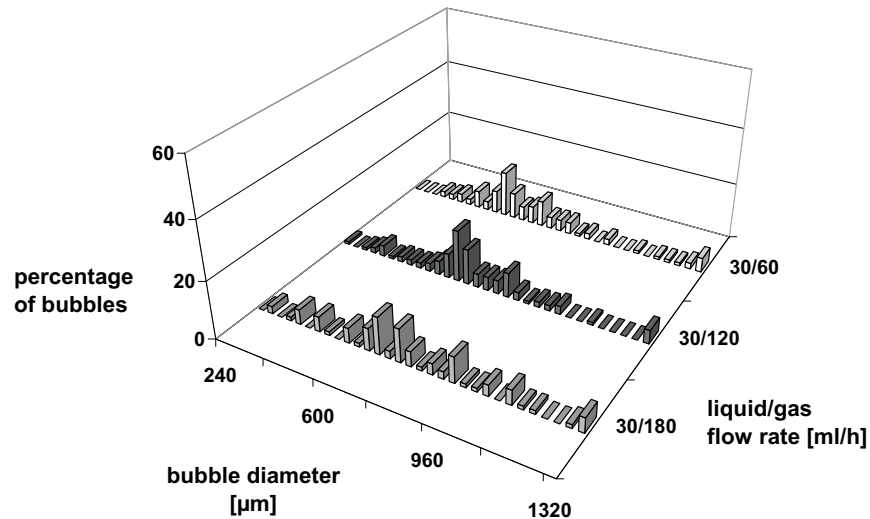


Fig. 9. Bubble size distribution for the triangular glass mixer.

To summarise the experiments, it can be stated that the geometry of the triangular glass micromixer, which was valuable for reducing lamellae thickness of one-phase liquid streams by geometric focusing [28,29], does not lead to a decrease of mean bubble diameter and broadness of BSD.

3.3. Foam formation in slit-shaped glass micromixer

At last, a set of experiments on foam formation was performed with the slit-shaped glass micromixer. Again, the liquid flow rate was kept constant at 30 ml/h while the gas flow rate was increased from 60 ml/h to 180 ml/min. Fig. 10 shows images of the bubble formation process and formed foam for selected experiments and allows direct comparison to the foams formed with the rectangular glass

micromixer. It is obvious that the slit-shaped geometry of the mixing chamber leads to essential smaller bubbles than with the rectangular or triangular glass micromixer. Even for high flow rates no big bubbles are formed. The geometry of the mixing chamber is more restricting in the proximity to the feed section than in the triangular glass micromixer. As a result, this extreme geometric constraint influences the bubbles directly and decisively during their formation rather than after their release. In the same way as for the experiments with the other mixers, not all gas feeding channels are active and the number of active gas feeding channels increases with the gas flow rate. The broadening of BSD with increasing gas flow rate becomes especially apparent when considering the images of the mixing chamber.

Flow rates	Slit-shaped glass mixer		For comparison: rectangular glass mixer
60 ml nitrogen/h 30 ml glycerol(aq)/h			
120 ml nitrogen/h 30 ml glycerol(aq)/h			
180 ml nitrogen/h 30 ml glycerol(aq)/h			

Fig. 10. Foam formation in slit-shaped glass mixer. The left row of images shows the flow through chamber, the middle row the glass tube connected to the mixer outlet. The right row shows as comparison the glass tube for the rectangular glass mixer. The liquid flow rate was kept constant at 30 ml/h while the gas flow rate was increased from 60 to 180 ml/h.

Totalling, the experiments with the glass micromixers have shown the following:

- Multi-channel gas feeding systems without design precautions specific for g/l-equipartition cause broadening of BSD.
- Geometry variations of the mixing chamber can be used to achieve smaller bubbles. Especially the slit-shaped geometry shows promising results.

The range of investigations with the glass micromixers was extended by conducting similar experiments with IMM's standard slit interdigital micromixer (SSIMM). As already mentioned, the geometry of the mixing chamber is determined by the same sequence of flow compression and expansion as in the mixing chamber of the slit-shaped glass micromixer. Within these experiments further variations of mixing chamber geometry and additionally a comparison between a multi-channel and a single-channel gas feeding systems were performed.

3.4. Foam formation in the standard slit interdigital micromixer with multi-channel gas feeding system

In the first set of experiments with SSIMM, the multi-channel gas feeding system was used. For constant gas and liquid flow rate, 60 and 30 ml/h, respectively, the height of the slit was varied from 30 to 180 μm . The left row of images in Fig. 11 shows the formed foams of these

experiments. Decreasing slit height from 120 to 30 μm , meaning increasing the geometric restrictions during bubble formation, leads to a steady decrease of mean bubble diameter. There are no major changes going from a slit height of 120–180 μm . This indicates that the slit height is no longer determinant for bubble size. As in the experiments with the glass mixers, the bubbles have no uniform size.

3.5. Foam formation in standard slit interdigital micromixer with single-channel gas feeding system

In the second set of experiments with SSIMM, the multi-channel gas feeding system was substituted by a single-channel gas feeding system. Deployed slit height and volume flows are the same as for the experiments with the multi-channel gas feeding system. The formed foams are shown in Fig. 11 (right row) and compared to the foams obtained with the multi-channel gas feeding system. Analogue to the first set of experiments, the mean bubble diameter decreases going from a slit height of 120 μm to a slit height of 30 μm and changes almost not for going from 120 to 180 μm slit height. But most important is that the mean bubble diameter and the broadness of the BSD are smaller in the case of the single-channel systems. This underpins strongly that a multi-channel gas feeding system without design precautions specific for g/l-equipartition broadens BSD and that a single-channel system circumvent this problem.

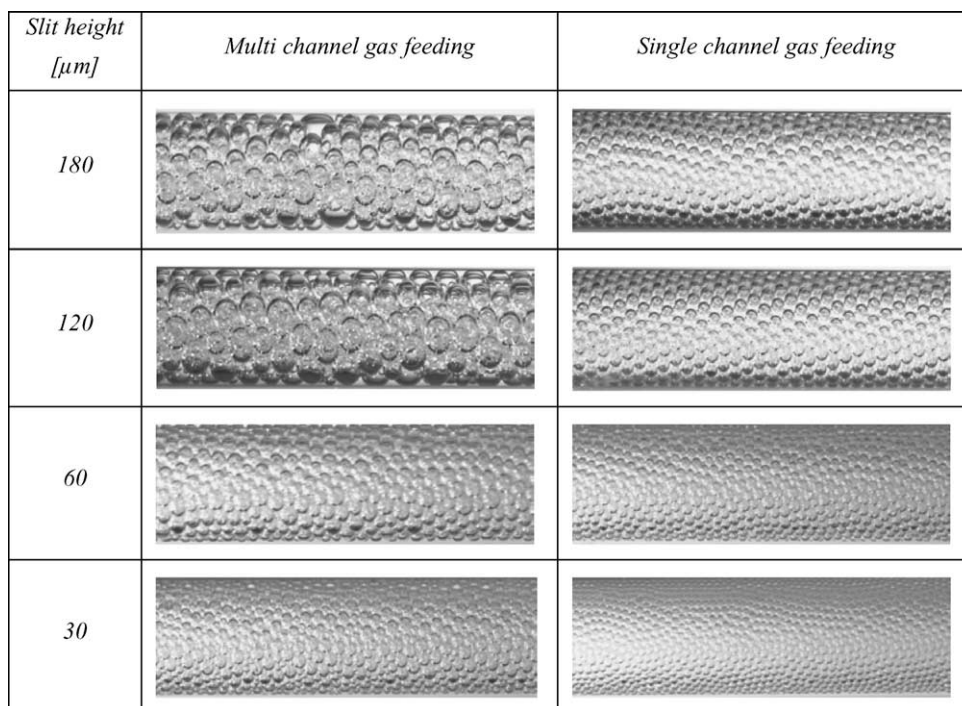


Fig. 11. Foam formation with IMM's standard slit interdigital micromixer. Variation of feeding system (multi- or single-channel gas feeding) and slit height (30, 60, 120 and 180 μm). Shown are the foams obtained in the glass tube connected to the outlet of the mixer. The flow rates were in each case 30 ml liquid/h and 60 ml nitrogen/h.

3.6. Incorporation of the single-channel gas feeding system in an experimental setup for serial screening

The investigations reported here serve to demonstrate the impact of having better-quality foams on a specific application. As already mentioned in the introduction, foams formed by SSIMM are also the basis for serial catalyst screening in g/l-systems described by de Bellefon et al. [24–26]. The basic principal thereby was to inject pulses of liquid containing either the catalyst or the reactant in the continuous liquid stream foamed in the micromixer with the gas. In the context of achieving a maximised number of experiments per time, investigations on residence time distribution and signal broadening linked with the foam formation were performed using the multi-channel gas feed system [30].

First experiments were now performed using the new single-channel gas feed system and compared to the corresponding experiments with the multi-channel gas feed system in regard to signal broadening [31]. Therefore, dye pulses were injected into the continuous liquid stream and the dimensionless exit age distribution functions $E(\theta)$ (θ is the dimensionless time defined as t/\bar{t} with \bar{t} as mean residence time) were determined at the outlet of the tube section by analysing concentration of the dye in the foam by UV-Vis spectroscopy after sampling. The experimental results show that the new single-channel gas feed system leads to a reduction of the dimensionless variance (see Fig. 12) and of the time spread of one signal at the outlet allowing to increase the maximum number of experiments per time, i.e. the improvement in hydrodynamics by specialised novel equipment does have an impact on a concrete application.

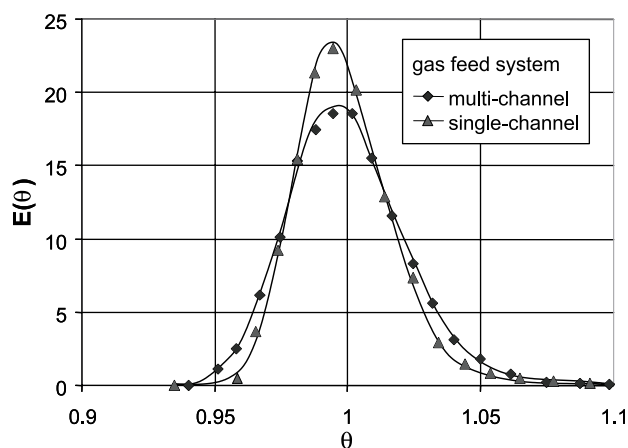


Fig. 12. Dimensionless exit age distribution function $E(\theta)$ of pulse broadening experiments based on IMM's standard slit interdigital micromixer (SSIMM) either equipped with a multi-channel or a single-channel gas feed system. The used system was nitrogen/water with sodium dodecyl sulphate (10^{-2} mol/kg) with a gas flow rate of 30 ml/h and a liquid flow rate of 10 ml/h.

4. Conclusions and outlook

Experiments with glass interdigital micromixers provided first basic insight in the bubble formation process in a multi-channel gas feeding system. As to be expected, no equipartition of gas was achieved in these mixers, which are multi-purpose tools for various mixing tasks. Consequently, the bubble formation process at the end of the gas feed channels was influenced strongly, resulting in non-uniform bubble sizes. Also, the mixing chamber geometry affects bubble size distribution and average bubble size. Here, the slit-shaped geometry with strong geometric restrictions for bubble formation and bubble pinch-off lead to the smallest bubbles and to a narrower BSD.

Experiments with IMM's standard slit interdigital micromixer (SSIMM) with analogous succession of flow compression and expansion zones in the mixing chamber as in the respective slit-shaped glass micromixer showed that the slit height is also an effective parameter to reduce bubble sizes. By changing the feeding structures from a multi-channel to a single-channel gas feed, the problem of non-equipartition was circumvented. The improvements achieved by the single-channel system are striking.

The main aim of the investigation described here was to get an overview about the impact of a broad range of factors influencing g/l-dispersion in interdigital micromixers. Only a few quantitative analyses of bubble sizes were performed. Systematic quantitative analyses and a broadening of experimental conditions like more extended variations of flow rates and flow rate ratios will allow a deeper understanding and are therefore tasks for the near future. The now investigated g/l-system leads to stable foams, i.e. coalescence is not changing foam quality. A further aspect of future work will be related to considering bubble merging, i.e. coalescence, in addition to bubble pinch-off and foam formation. However, this foam stability is only achieved by the restraint of adding surfactant and the limitation to aqueous systems. In turn, bursting out these restrictions implies the knowledge on and the handling of fast coalescence in g/l-systems.

It is obvious that the introduced single-channel gas feeding systems is in close neighbourhood to other systems (simple microstructured T-junctions or the use of micro-capillaries in a tube in tube device). It is certainly worth working out the differences between these systems and their potentials with the aim to identify for each application the most advantageous system.

Acknowledgements

The authors thank for funding of this work through the German Volkswagen Stiftung (reference number I/75680) and the European Commission (EU project "Key Elements for the Application of Microreactors in Multiphasic Catalytic Chemistries (KEMiCC)" (GRD1-2000-2562).

References

- [1] V. Haverkamp, W. Ehrfeld, K. Gebauer, V. Hessel, H. Löwe, T. Richter, C. Wille, The potential of micromixers for contacting of disperse liquid phases, *Fresen. J. Anal. Chem.* 364 (1999) 617–624.
- [2] P.B. Umbanhowar, V. Prasad, D.A. Weitz, Monodisperse emulsion generation via drop break off in coflowing stream, *Langmuir* 16 (2) (2000) 347–351.
- [3] A.M. Ganan-Calvo, Generation of steady liquid microthreads and micron-sized monodisperse sprays in gas streams, *Phys. Rev. Lett.* 80 (2) (1998) 285–288.
- [4] S. Sugiura, M. Nakajima, M. Seki, Monodispersed droplet formation caused by interfacial tension from microfabricated channel array, in: M. Matlosz, W. Ehrfeld, J.P. Baselt (Eds.), *Proceedings of the Fifth International Conference on Microreaction Technology (IMRET-5)*, Springer-Verlag, Berlin, 2001, pp. 252–261.
- [5] S. Hardt, F. Schönfeld, F. Weise, C. Hofmann, V. Hessel, W. Ehrfeld, Mixing and emulsification processes in micromixers, in: *Proceedings of the Computational Methods for Multiphase Flow*, Orlando, USA, 14–16 March 2001, pp. 217–228.
- [6] F. Schönfeld, D. Rensink, Simulation of droplet generating by mixing nozzles, *Chem. Eng. Technol.* 26 (2003) 5.
- [7] J. Eggers, Nonlinear dynamics and breakup of free-surface flows, *Rev. Modern Phys.* 69 (3) (1997) 865–929.
- [8] S. Freitas, A. Walz, H.P. Merkle, B. Gander, Solvent extraction employing a static micromixer: a simple, robust and versatile technology for the microencapsulation of proteins, *J. Microencapsulation* 20 (1) (2003) 67–85.
- [9] C. Erni, C. Suard, S. Freitas, D. Dreher, H.P. Merkle, E. Walter, Evaluation of cationic solid lipid microparticles as synthetic carriers for the targeted delivery of macromolecules to phagocytic antigen-presenting cells, *Biomaterials* 23 (2002) 4667–4676.
- [10] C. Mahe, J.F. Tranchant, J. Burgold, N. Schwesinger, A microstructured device for the production of emulsions on demand, in: *Proceedings of the Sixth International Conference on Microreaction Technology (IMRET-6)*, AIChE Pub. No. 164, New Orleans, USA, 11–14 March 2002, pp. 159–167.
- [11] K. Benz, K.-J. Regenauer, K.-P. Jäckel, J. Schiewe, W. Ehrfeld, H. Löwe, V. Hessel, Utilisation of micromixers for extraction processes, *Chem. Eng. Technol.* 24 (1) (2001) 11–17.
- [12] A. Ganan-Calvo, J.M. Gordillo, Perfectly monodisperse microbubbling by capillary flow focusing, *Phys. Rev. Lett.* 87 (27) (2001) 274501–274504.
- [13] V. Hessel, W. Ehrfeld, K. Golbig, V. Haverkamp, H. Löwe, T. Richter, Gas/liquid dispersion processes in micromixers: the hexagon flow, in: W. Ehrfeld, I.H. Rinard, R.S. Wegeng (Eds.), *Process Miniaturization: Second International Conference on Microreaction Technology (IMRET-2)*, Topical Conference Preprints, AIChE, New Orleans, USA, 1998, pp. 259–266.
- [14] V. Hessel, W. Ehrfeld, T. Herweck, V. Haverkamp, H. Löwe, J. Schiewe, C. Wille, T. Kern, N. Lutz, Gas/liquid microreactors: hydrodynamics and mass transfer, in: *Proceedings of the Fourth International Conference on Microreaction Technology (IMRET-4)*, AIChE Topical Conference Proceedings, Atlanta, USA, 5–9 March 2000, pp. 174–186.
- [15] V. Hessel, W. Ehrfeld, K. Golbig, V. Haverkamp, H. Löwe, M. Storz, C. Wille, A. Guber, K. Jähnisch, M. Baerns, Gas/liquid microreactors for direct fluorination of aromatic compounds using elemental fluorine, in: W. Ehrfeld (Ed.), *Proceedings of the Third International Conference on Microreaction Technology (IMRET-3)*, Springer-Verlag, Berlin, 2000, pp. 526–540.
- [16] V. Haverkamp, G. Emig, V. Hessel, M.A. Liauw, H. Löwe, Characterization of a gas/liquid microreactor, the microbubble column: determination of specific interfacial area, in: M. Matlosz, W. Ehrfeld, J.P. Baselt (Eds.), *Proceedings of the Fifth International Conference on Microreaction Technology (IMRET-5)*, Springer-Verlag, Berlin, 2001, pp. 202–214.
- [17] M.W. Losey, R.J. Jackman, S.L. Firebaugh, M.A. Schmidt, K.F. Jensen, Design and fabrication of microfluidic devices for multiphase mixing reaction, *J. Microelectromech. Syst.* 11 (6) (2002) 709–717.
- [18] M.W. Losey, M.A. Schmidt, K.F. Jensen, Microfabricated multiphase packed-bed reactors: characterization of mass transfer and reactions, *Ind. Chem. Res.* 40 (2001) 2555–2562.
- [19] M.W. Losey, M.A. Schmidt, K.F. Jensen, A micro packed-bed reactor for chemical synthesis, in: W. Ehrfeld (Ed.), *Proceedings of the Third International Conference on Microreaction Technology (IMRET-3)*, Springer-Verlag, Berlin, 2000, pp. 277–286.
- [20] W. Ehrfeld, V. Hessel, H. Löwe, *Micromixers*, VCH, Weinheim, 2000.
- [21] W. Ehrfeld, K. Golbig, V. Hessel, H. Löwe, T. Richter, Characterization of mixing in micromixers by a test reaction: single mixing units and mixer arrays, *Ind. Eng. Chem. Res.* 38 (3) (1999) 1075–1082.
- [22] H. Löwe, W. Ehrfeld, V. Hessel, T. Richter, J. Schiewe, Micromixing technology, in: *Proceedings of the Fourth International Conference on Microreaction Technology (IMRET-4)*, AIChE Topical Conf. Proc., Atlanta, USA, 5–9 March 2000, pp. 31–47.
- [23] H. Mathes, P.J. Plath, Generation of monodisperse foams using a microstructured static mixer, in: *Proceedings of the Tunisian–German Conference of Smart Systems and Devices*, Hammamet, Tunisia, 27–30 March 2001, submitted for publication.
- [24] C. de Bellefon, N. Tanchoux, S. Caravieilles, P. Grenouillet, V. Hessel, Microreactors for dynamic high throughput screening of fluid-liquid molecular catalysis, *Angew. Chem.* 112 (19) (2000) 3584–3587.
- [25] C. de Bellefon, N. Pestre, T. Lamouille, P. Grenouillet, High-throughput kinetic investigations of asymmetric hydrogenations with microdevices, *Adv. Synth. Catal.* 345 (1–2) (2003) 190–193.
- [26] C. de Bellefon, R. Abdallah, T. Lamouille, N. Pestre, S. Caravieilles, P. Grenouillet, High-throughput screening of molecular catalysts using automated liquid handling, injection and microdevices, *Chimia* 56 (11) (2002) 621–626.
- [27] T. Herweck, S. Hardt, V. Hessel, H. Löwe, C. Hofmann, F. Weise, T. Dietrich, A. Freitag, Visualization of flow patterns and chemical synthesis in transparent micromixers, in: M. Matlosz, W. Ehrfeld, J.P. Baselt (Eds.), *Proceedings of the Fifth International Conference on Microreaction Technology (IMRET-5)*, Springer-Verlag, Berlin, 2001, pp. 215–229.
- [28] V. Hessel, S. Hardt, H. Löwe, F. Schönfeld, Laminar mixing in different interdigital micromixers—Part I: experimental characterization, *AIChE J.* 49 (3) (2003) 566–577.
- [29] S. Hardt, F. Schönfeld, Laminar mixing in different interdigital micromixers—Part 2: numerical simulations, *AIChE J.* 49 (3) (2003) 578–584.
- [30] H. Pennemann, V. Hessel, H.-J. Kost, H. Löwe, C. de Bellefon, Investigations on pulse broadening for transient catalyst screening in gas/liquid systems, *AIChE J.* (2004) accepted.
- [31] H. Pennemann, V. Hessel, H.-J. Kost, H. Löwe, C. de Bellefon, N. Pestre, T. Lamouille, P. Grenouillet, High-throughput experimentation with a micromixer based, automated serial screening apparatus for polyphasic fluid reactions, in: *Proceedings of the International Conference on Process Intensification for the Chemical Industry*, Maastricht, The Netherlands, 13–15 October 2003, pp. 137–147.